ADV MATH SCI JOURNAL
Advances in Mathematics: Scientific Journal **10** (2021), no.3, 1357–1370
ISSN: 1857-8365 (printed); 1857-8438 (electronic)
https://doi.org/10.37418/amsj.10.3.23

HEAT AND MASS TRANSFER ANALYSIS OF CASSON FLUID FLOW OVER A MOVING WEDGE FILLED WITH NANOFLUID

N. Amar[1] and N. Kishan[2]

ABSTRACT. The flow, heat and mass transfer behaviour of Casson fluid over a movable wedge embedded in porous medium in existence of thermal radiation, Brownian motion, thermophoresis, permeability and Prandtl number is explained in detailed. The system of nonlinear partial differential equations are changed into nonlinear ordinary differential equations by using similar transformations. The outcome ordinary differential equations are solved by the familiar bvp4c shooting technique for three different cases: (i) the flow over static wedge ($\Lambda = 0$), (ii) the wedge moves along the flow ($\Lambda > 0$) and (iii) the wedge moves opposite the flow ($\Lambda < 0$). After plotting the obtained numerical results of all the non-dimensional physical parameters on the profiles of velocity, temperature and concentration are described in detailed. The variations of skin friction, Nusselt number and Sherwood number is also analyzed.

1. INTRODUCTION

The cooling efficiency of traditional fluids such as water and oil is reduced due to low thermal conductivity. Furthermore, the angle of wedge plays a crucial role in studying transonic flow on aerodynamic surfaces and wings, as

[1]*corresponding author*

2020 *Mathematics Subject Classification.* 76-10, 80-10.

Key words and phrases. Thermal radiation, MHD, Moving Wedge, Melting parameter, Casson nanofluid, Porous media.

Submitted: 01.01.2021; *Accepted:* 16.01.2021; *Published:* 18.03.2021.

mentioned by Jamson [1]. Kumari et.al. [2] investigated on mixed convection flow with magnetic effect over a wedge embedded in a highly porous medium. Cheng [3] studied the numerically examine the melting influence on transient heat transfer from a vertical plate in a liquid saturated porous media. Choi [4] has shown that this limited cooling performance can be Specified by adding to the traditional fluid a small extent of high heat transfer behaviour of nano-solid particles to form so-called nanofluids. The particles in these nanofluids vary from 1 to 100 nm and are in the form of oxides, carbides, metals, nitrides or non-metals. Nanofluid has more than a few technical and physical applications for heat transfer, for examples cooling of engines, chillers, refrigerators, fuel cells, etc. Since, then many researchers have studied various properties of nanofluid such as thermophysical property, thermal instability and inclination angle under different conditions. Furthermore, Gorla et al. [5] in the circular stretch cylinder in the nanofluid, the problems of mixed convection over the vertical wedge and heat transfer in the boundary layer were studied. Falkner and Skan [6] a viscous fluid flow exceeding the static wedge using a similarity transformation was first developed. In recent years, authors have shown an interest in the Falkner-Skan flow by taking into account different parameter effects. In addition, Lin and Lin [7] measured the continuous flow of two-dimensional laminar heat transfer from a wedge. Kandasamy et.al. [8] discussed the heat and mass transfer along a wedge with effect of the source/suction and chemical reaction. In past years, several studies have been carried out into a fluid influenced by a magnetic field, one of the reasons why it is widely used in medical and industrial applications. Recently, MHD flow with mass transfer and heat over porous media have been extensively taken into account as a consequence of their critical applications in numerous engineering processes such as liquid metal filtration, metallurgy, cooling of nuclear reactors, etc. However, very few investigations on nanofluid flows of Casson MHD in a permeable medium and the relevant research is mentioned [9, 10]. Several authors are researched on different fluid aspects viz,. [11–16].

Motivated by the above studies, we initiated a new work heat and mass transfer investigation of Casson fluid flow on movable wedge filled with nanofluid over porous medium. For the numerical solution we used bvp4c shooting procedure. For velocity, temperature and concentration profiles, for different physical

parameters we analyzed. We also use the above mentioned technique to tabulate the values of Skin friction, Nusselt number and Sherwood number.

2. Formulation of mathematics

Considering an incompressible two-dimensional steady with forced convection Casson nanofluid flow beyond a movable wedge embedded in a porous medium with the effect of thermal radiation. Suppose the induced magnetic field is very low and therefore ignored. The velocity at the wedge and the external flow (free flow) are: $u_w(x) = U_w x^m$ and $U(x) = u_i(x) = a_i x^m$, where a_i denotes +ve real constant. Nanopartical volumetric friction is C_w and T_m is the surface temperature due to melting. In addition, assume magnetic field $B(x) = B_0 x^m, B_0$ is the fixed magnetic field and is employed to be normal to the wall of the wedge.

Similarly, the permeability of the support is assumed to be type of $K(x) = Kx^m, K'$ is the nondimensional permeability and $m = \frac{\beta_1}{2-\beta_1}$ such that $m, \quad \beta_1$ and Ω represent the angle of wedge, the Hartree pressure gradient and the total wedge angle, respectively.

We take $m \in [0, 1].T_\infty$ temperature and C_∞ concentration far away from the surface. Here $T_m < T_\infty$ and, $T_m > T_0$ having in mind all the above assumption.

$$\frac{\partial u}{\partial x} + \frac{\partial v}{\partial y} = 0 \tag{2.1}$$

$$\begin{aligned} &u\frac{\partial u}{\partial x} + v\frac{\partial u}{\partial y} \\ &= u_i(x)\left(\frac{\partial u_i}{\partial x}\right) + \vartheta\left(1 + \frac{1}{\beta}\right)\frac{\partial^2 u}{\partial y^2} + \left(\frac{\sigma B^2(x)}{\rho_f} + \frac{\vartheta}{k(x)}\right)(u_i(x) - u) \end{aligned} \tag{2.2}$$

$$u\frac{\partial T}{\partial x} + v\frac{\partial T}{\partial y} = \alpha\frac{\partial^2 T}{\partial y^2} + \tau\left[D_B\frac{\partial C}{\partial y}\frac{\partial T}{\partial y} + \frac{D_\tau}{T_\infty}\left(\frac{\partial T}{\partial y}\right)^2\right] - \frac{1}{(\rho c_p)}\frac{\partial q_r}{\partial y} \tag{2.3}$$

$$u\frac{\partial C}{\partial x} + v\frac{\partial C}{\partial y} = D_B\frac{\partial^2 C}{\partial y^2} + \frac{D_T}{T_\infty}\frac{\partial^2 T^2}{\partial y^2} \tag{2.4}$$

Here (u, v) be the velocity components along x and y-axis respectively, T is the nanofluid temperature, C indicate the nanoparticle concentration, D_B indicates the Brownian diffusion coefficient, D_T coefficient of thermophoresis diffusion, σ

is the electrical conductivity, ϑ is the nanofluid viscosity, $\alpha = \frac{k}{\rho c_f}$ is the thermal diffusivity $\tau = \frac{\rho C_p}{\rho C_f}$ is the ratio of nanoparticle heat capacity to the base fluid, β is the Casson parameter, heat capacitance $(\rho C_p)_f$ and the effective density ρ_f.

The related boundary conditions are:

$$\begin{aligned} &u = u_w(x) = U_w x^m, \quad v = 0, \\ &K\frac{\partial T}{\partial y} = \rho_f \left[\lambda + C_s\left(T_m - T_0\right)\right] v(x,0), T = T_m, C = C_w \text{ at } y = 0\} \end{aligned} \tag{2.5}$$

$$u \to U(x), v = 0, T \to T_\infty, C \to C_\infty, \text{ as } y \to \infty. \tag{2.6}$$

Here k is thermal conductivity, λ is the latent heat, T_0 is solid surface temperature, ρ is density, and C_s be solid surface heat capacity. Applying the Rosseland approximation, the radiation heat flux is specified as:

$$q_r = \frac{4\sigma_i}{3K^*}\frac{\partial T^4}{\partial y}. \tag{2.7}$$

Here, σ_i mentions Stefan-Boltzmann constant, K^* specify the coefficient of mean absorption, and T^4 is linear sum of the temperature and it can be extended together with T_∞ the assistance of the Taylor series:

$$T^4 = T_\infty^4 + 4T_\infty^3\left(T - T_\infty\right) + 6T_\infty^2\left(T - T_\infty\right)^2 + \ldots. \tag{2.8}$$

Neglecting higher order term of $T - T_\infty$ onward of Eq.(2.8) we achieve:

$$T^4 \cong 4TT_\infty^3 - 3T_\infty^3. \tag{2.9}$$

From solving Eqs. (2.7) and (2.9) we get:

$$q_r = -\frac{16T_\infty^3\sigma_i}{3K^*}\frac{\partial T}{\partial y}. \tag{2.10}$$

Rewrite the Eq.(2.3), by the help of Eq.(2.10) is given:

$$u\frac{\partial T}{\partial x} + v\frac{\partial T}{\partial y} = \alpha\frac{\partial^2 T}{\partial y^2} + \tau\left[D_B\frac{\partial C}{\partial y}\frac{\partial T}{\partial y} + \frac{D_T}{T_\infty}\left(\frac{\partial T}{\partial y}\right)^2 + \frac{16T^3{}_\infty\sigma_i}{3\left(\rho C_p\right)_f K^*}\frac{\partial^2 T}{\partial y^2}\right], \tag{2.11}$$

and introduce the similarity transformation are as follows:

$$\begin{aligned} \psi &= \left(\frac{2x\vartheta a_i x^m}{m+1}\right)^{\frac{1}{2}} \mathrm{f}(\eta), \quad \eta = y\left(\frac{(m+1)a_i x^m}{2x\vartheta}\right)^{\frac{1}{2}}, \\ \theta(\eta) &= \frac{T - T_m}{T_\infty - T_m}, \phi(\eta) = \frac{C - C_\infty}{C_w - C_\infty}. \end{aligned} \tag{2.12}$$

Now, define $u = \frac{\partial \psi}{\partial y}$ and $v = -\frac{\partial \psi}{\partial x}$ so as to be identically satisfy Eq.(2.1). Substituting Eq.(2.12) in Eq.(2.2), Eq.(2.4) and Eq.(2.11), then we get non linear ordinary differential equations:

$$\left(1+\frac{1}{\beta}\right) f''' + \frac{2m}{m+1}\left(1-(f')^2\right) + ff'' + \left(M+\frac{1}{K_p}\right)(1-f') = 0, \tag{2.13}$$

$$\left(1+\frac{4R}{3}\right)\theta'' + Pr\left(f\theta' + Nb\theta'\phi' + Nt(\theta')^2\right) = 0, \tag{2.14}$$

$$\phi'' + \frac{Nt}{Nb}\theta'' + Le\phi' f = 0. \tag{2.15}$$

Rewrite the above boundary conditions Eq.(2.5) and Eq.(2.6) are given bellow:

$$\left.\begin{array}{c} f'(\eta) = \Lambda, \theta(\eta) = 0, \emptyset(\eta) = 1, B'\theta'(\eta) + \mathrm{Prf}(\eta) = 0, \text{ at } \eta = 0 \\ f'(\eta) \to 1, \theta(\eta) \to 1, \emptyset(\eta) \to 0, \text{ as } \eta \to \infty \end{array}\right\} \tag{2.16}$$

Here prime denote the derivative with respect to η, $\frac{4T^3\infty\sigma_i}{3KK^*}$ is the radiative parameter, $Pr = \frac{\vartheta}{\alpha}$ is the Prandtl Number, $\Lambda = \frac{U_w}{a_i}$ indicates the ratio of the wall velocity to the free stream fluid velocity, $B' = \frac{c_{f(T_\infty - T_m)}}{\lambda + C_S(T_m - T_0)}$ is the melting parameter, here $\frac{c_{f(T_\infty - T_m)}}{\lambda}$ and $\frac{C_S(T_m - T_0)}{\lambda}$ are the Stefan number for the liquid state and solid state, respectively. $M = \frac{2\sigma B_0^2}{\rho_f a_i(m+1)}$ is the magnetic field parameter, $k_p = \frac{a_i k'(m+1)}{2\vartheta}$ is the permeability parameter, $Nt = \frac{D_T(T_\infty - T_m)\tau}{\vartheta T_\infty}$ is the thermophoresis parameter, $Nb = \frac{D_B(C_W - C_\infty)\tau}{\vartheta}$ is the Brownian parameter, $Le = \frac{\vartheta}{D_B}$ is the Lewis number, and f', θ and ϕ are the dimensionless velocity, temperature and concentration profiles respectively.

Practical importance of the problem is the shear stress rate C_f, heat transfer rate Nu_x and mass transfer rate Sh_x are expressed as:

$$C_f = \frac{\tau_w}{\rho_f u_e^2}, \tau_w = \mu_B\left(1+\frac{1}{\beta}\right)(u_y)_{y=0},$$

$$Nu_x = \frac{xq_w}{k\left(T_\infty - T_m\right)}, \quad q_w = -K\left(T_y\right)_{y=0} + q_r,$$

$$Sh_x = \frac{xq_m}{D_B\left(C_w - c_\infty\right)}, q_m = -D_B\left(C_y\right)_{y=0}.$$

Therefore, the dimensionless Skin friction quantity, Nusselt and Sherwood numbers are expressed respectively as given below:

$$\left(\frac{2}{m+1}Re\right)^{\frac{1}{2}} C_f = \left(1+\frac{1}{\beta}\right) f''(0);$$

$$\left(\frac{2}{m+1}Re\right)^{\frac{1}{2}} Nu_x = -(1+4R)\theta'(0);$$

$$\left(\frac{2}{m+1}Re\right)^{\frac{1}{2}} Sh_x = -\phi'(0).$$

Here, the local Reynolds number $Re = \frac{xu_i(x)}{\vartheta}$

3. Numerical approach

The transformed system of Eqs.(2.13)-(2.15) and the boundary conditions (2.16) have been solved numerically by using the bvp4c shooting technique. Compare with other numerical methods, the bvp4c technique is more versatile and finer to control approach criteria. The programming scheme contains the following points.

Reducing the Eqs.(2.13)-(2.15) in to system of first-order equations via suitable substitution defined as following:

$$\begin{array}{l} f(1) = f(\eta), \quad f(2) = f'(\eta), \quad f(3) = f''(\eta), \\ f(4) = \theta(\eta), \quad f(5) = \theta'(\eta), f(6) = \emptyset(\eta), \quad f(7) = \emptyset'(\eta). \end{array}$$

Now we get a first-order system of equation:

$$\begin{pmatrix} f'(1) \\ f'(2) \\ f'(3) \\ f'(4) \\ f'(5) \\ f'(6) \\ f'(7) \end{pmatrix} = \begin{pmatrix} f(2) \\ f(3) \\ \left(\frac{-1}{1+\frac{1}{\beta}}\right)\left(\frac{2m}{m+1}\left(1-f(2)^2\right)+f(1)f(3)+\left(M+\frac{1}{K_p}\right)(1-f(2))\right) \\ f(5) \\ \frac{-1}{1+\frac{4R}{3}}\left(\Pr\left(f(1)f(5)+Nbf(5)f(7)+Ntf(5)^2\right)\right) \\ f(7) \\ \frac{Nt}{Nb}\left(\frac{1}{1+\frac{4R}{3}}\right)\left(\Pr\left(f(1)f(5)+Nbf(5)f(7)+Ntf(5)^2\right)\right)-\mathrm{Lef}(7)f(1) \end{pmatrix}.$$

The associated initial conditions are:

$$\begin{pmatrix} f_a(1) \\ f_a(2) \\ f_a(4) \\ f_a(6) \\ f_b(2) \\ f_b(4) \\ f_b(6) \end{pmatrix} = \begin{pmatrix} \frac{-1}{Pr} B' f_a(5) \\ \Lambda \\ 0 \\ 1 \\ 1 \\ 1 \\ 0 \end{pmatrix}$$

- Use the boundary conditions to build three unknowns.
- The method will be repeated until the requirement is reached asymptotically converged.

3.1. **Validation of program:**

3.1.1. *Table 1:* The values of the skin friction $f''(0)$ when $M = 0, Nb = 0.001, Nt = 0, Le = 1, Kp \to \infty, m = 0, \beta \to \infty, \Pr = 1, R = 0, \Lambda = 0$. For distinguish of B' with existing results the following comparison are:

TABLE 1.

B'	Ishak [15]	Subharthi Sarkar [16]	Presented Result
0	0.4696	0.4696	0.469601
1	0.2790	0.2790	0.279037
2	0.2019	0.2022	0.202243
4	0.1594	0.1598	0.159762

To examine the exactness of our current program, we have compile the captured outcomes of the Skin friction factor $f''(0)$, for numerous values of melting parameter B'. We have executed the same numerical program in the non-appearance of magnetic field parameter, thermal radiation and thermophoresis factor. It is mentioned that our results were favorable with a maximum percentage error 0.001 only. Which means that our results are very close to Ishak [15] and Subharthi Sarkar [16] as presented in Table 1. Hence, the code used here is honest and effective for computing.

4. Results and Discussion

The transformed system of equations and subject to the equivalent boundary conditions are resolved numerically by use of bvp4c shooting technique. To examine the output these numerical solutions through the non-dimensional existing parameters on the flow, heat & mass transfer of Casson nanofluid flow over a wedge. For the numerical calculation, we set the nondimensional values as follows: $\beta = 2, \mathrm{M} = 0.5, \mathrm{R} = 0.8, B' = 1,\ \mathrm{m} = 0.2, \mathrm{Pr} = 1, K_p = 0.5, \mathrm{Le} = 1, \mathrm{Nb} = 0.6$. These values are kept same throughout the study excluding the distinct values that are used in particular figures and tables. In the current review, $\Lambda = 0$ specifies the flow over fixed wedge, $\Lambda < 0$ specifies the wedge moving in the reverse direction, $\Lambda > 0$ specifies wedge moving in the same direction.

From the Table 2, It can be observed that in the existence of magnetic field parameter, the Skin friction value attains maximum in all three cases. We observed that the coefficient of friction factor is unusually low in the case of $\Lambda > 0$, and when to slow down the friction between the particles, in the case of $\Lambda > 0$. Exactly the inverse behaviour was observed in the case of the Casson parameter. We have also saw that the mass transfer and heat transfer rates are enhanced with the increasing in Casson parameter and the reverse behaviour was observed in the magnetic field parameter. Heat and mass transfer rates are large in $\Lambda > 0,$ when compared to the remaining cases $\Lambda = 0$ and $\Lambda < 0$. We conclude that declining heat and mass transfer rates is useful to encourage it for $\Lambda > 0$.

Figure 1 explains the influence of the wedge angle m on the velocity profile for distinct of Λ. This would be noticeable, the velocity curves improves as the wedge angle variations for $\mathrm{m} = 0.2, 1, 5$ in choice of Λ. It is also apparent from this figure that large values of m shorting the speed of the thickness of the limit layer when $\Lambda > 0$ with respect to the case $\Lambda = 0$ and $\Lambda < 0$. The impact of m on velocity is more prominent in the case of $\Lambda < 0$. The deviation of the fluid velocity from the nanofluid parameter of β for several cases of Λ, as shown in Fig.2.

We begin to think that the increment of the nanofluid parameter β reduces the velocity profile, since the nanofluid parameter of Casson is directly proportional to the dynamic viscosity. i.e., increasing the parameter of the nanofluid of Casson increases the viscosity, which outcomes are decline of the fluid velocity.

TABLE 2. Obtain the values of Skin friction, Nusselt and Sherwood numbers with non-dimensionless parameters for different cases of Λ

β	m	Kp	Pr	Nb	Nt	Le	B'	R	M	$f''(0)$			$-\theta''(0)$			$-\phi'(0)$		
										Λ=0	Λ>0	Λ<0	Λ=0	Λ>0	Λ<0	Λ=0	Λ>0	Λ<0
2										2.4542	1.9907	2.9034	2.0245	2.0871	1.9605	0.4047	0.4329	0.3761
4										1.8847	1.5287	2.2297	2.0047	2.0713	1.9366	0.3976	0.4273	0.3676
	0.1									2.2781	1.8434	2.7020	1.9310	1.9923	1.8683	0.3848	0.4123	0.3569
	0.3									2.6186	2.1280	3.0920	2.1135	2.1714	2.0480	0.4236	0.4525	0.3942
		1								2.0534	1.6753	2.4142	1.9874	2.0589	1.9135	0.3910	0.4225	0.3588
		2								1.8241	1.4959	2.1327	1.9619	2.0399	1.8807	0.3818	0.4156	0.3471
			2							2.5428	2.0627	3.0081	2.5879	2.6924	2.4812	0.4828	0.5172	0.4478
			4							2.6075	2.1157	3.0838	3.1059	3.2681	2.9400	0.5457	0.5887	0.5020
				0.6						2.3671	1.9204	2.8001	1.6609	1.7022	1.6185	0.3421	0.3671	0.3169
				0.8						2.4190	1.9623	2.8618	1.8572	1.9097	1.8036	0.3780	0.4047	0.3511
					0.2					2.4542	1.9907	2.9034	2.0245	2.0871	1.9605	0.4047	0.4329	0.3761
					0.6					2.4476	1.9854	2.8956	2.0799	2.1431	2.0152	0.5045	0.5458	0.4627
						1				2.4542	1.9907	2.9034	2.0245	2.0871	1.9605	0.4047	0.4329	0.3761
						3				2.4553	1.9917	2.9046	2.0152	2.0768	1.9522	0.4204	0.4697	0.3711
							2.5			2.2034	1.7834	2.6129	1.6997	1.7540	1.6442	0.2460	0.2667	0.2251
							4.5			1.9911	1.6077	2.3669	1.4151	1.4617	1.3675	0.1321	0.1463	0.1181
								2		2.4542	1.9907	2.9034	2.0245	2.0871	1.9605	0.4047	0.4329	0.3761
								3		2.4740	2.0079	2.9254	2.6844	2.7565	2.6105	0.4259	0.4556	0.3958
									2	2.8028	2.2663	3.3270	2.0509	2.1074	1.9934	0.4148	0.4407	0.3886
									4	3.4018	2.7413	4.0522	2.0871	2.1356	2.0381	0.4240	0.4518	0.4062

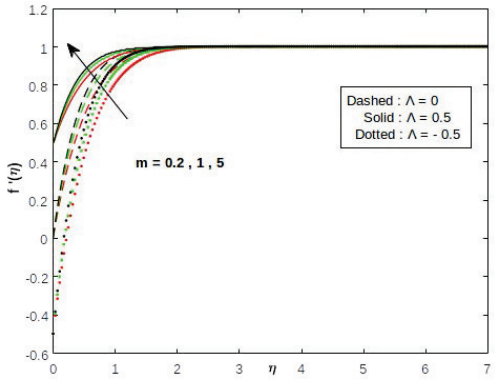

FIGURE 1. Influence of m on velocity for various values of Λ

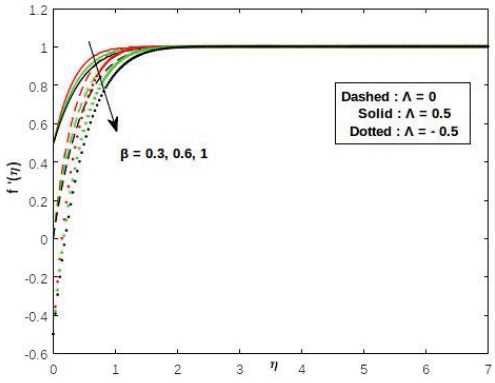

FIGURE 2. Influence of β on velocity for various values of Λ

Fig. 3 depict the influence of the magnetic field on the velocity profile. Now, from the figure, we conclude that, the width of the boundary layer reduced with a rising the magnetic parameter in the three cases $\Lambda > 0, \Lambda = 0$ and $\Lambda < 0$.

That is, the velocity profile goes up to the free flow rate that proceeds an upper field strength. Henceforth the magnetic field improve the magnitude of the nanofluid velocity. Fig. 4 depict the consequence of K_p on the velocity profile. It is pointed out that the velocity curves decline with an rise in K_p. That is why the velocity of nanofluids tends to the free flow rate for increased values of K_p. The inverse influence of K_p in the velocity profile corresponds to the earlier effect of the magnetic field. From this Fig. 5 and Fig. 6 it can be viewed that the radiation parameter values enhance, the temperature and concentration curves are decreasing.

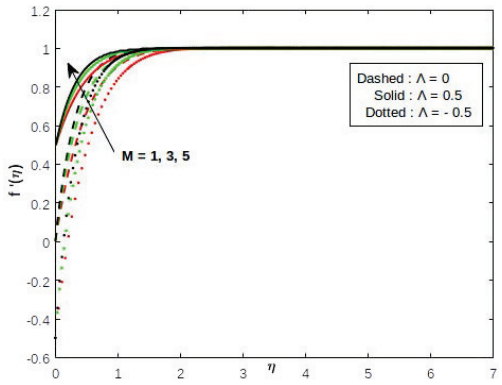

FIGURE 3. Influence of M on velocity for various values of Λ

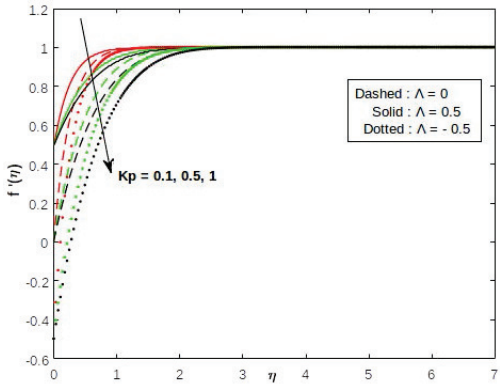

FIGURE 4. Influence of Kp on velocity for various values of Λ

The behavior of Brownian motion on temperature distribution is depicted in Fig.7. We can observe that as values of Nb goes up, the temperature profiles goes down. Physically, the Brownian motion is a random flow of tiny particles deferred in a fluid as an outcome of its collision with the quick movement of particles in the nanofluid. That type a collision improves the melting method, the melting procedure that produces more nanofluids in the system, resulting in the reducing of temperature profile. Fig.8 depicts the enhance of the Brownian motion parameter, the concentration curves increases throughout the flow domain. Fig.9 represents the influence of Prandtl number on the temperature field. In this study of heat transfer, the corresponding thickness of the thermal boundary layer can be managing by the Prandtl number. Therefore, when the Prandtl number is maximum, the heat diffuses decreases. This intends that for a large value of Prandtl number the thermal boundary layer is the thickness

is very little. Consequently, as the Prandtl Number rises, thermal diffusion decline, which inhibits the melting method. This leads the enhance of temperature profile with the Prandtl number.

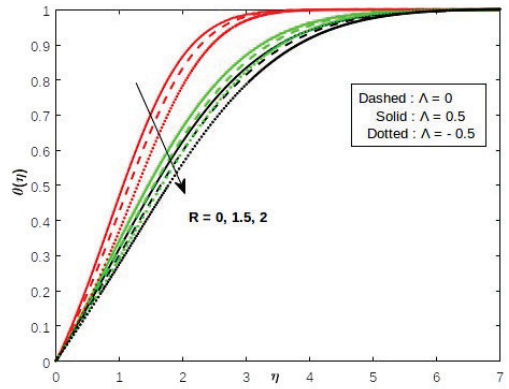

FIGURE 5. Influence of Kp on Temperature for various values of Λ

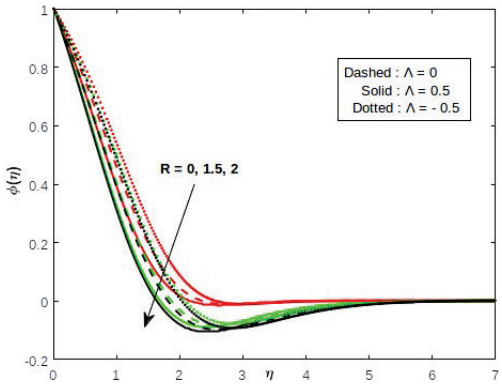

FIGURE 6. Influence of R on concentration for various values of Λ

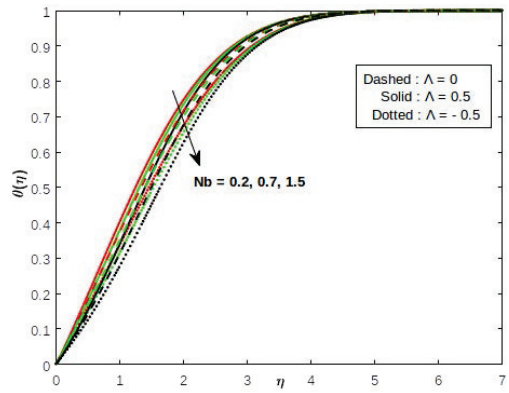

FIGURE 7. Influence of Nb on Temperature for various values of Λ

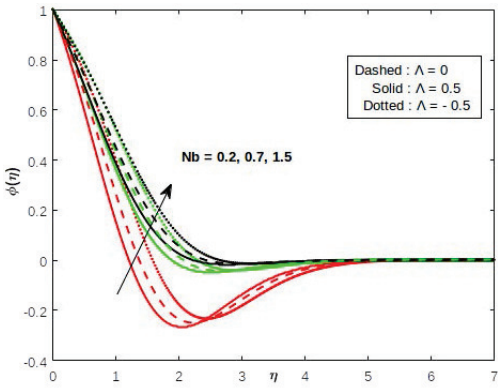

FIGURE 8. Influence of Nb on concentration for various values of Λ

Fig.10 depicts decline the concentration profile increases the Lewis Number. Fig.11 we notice that the concentration profile falls with the rise the thermophoresis values. Fig.12 explains the effect of thermophoresis on temperature

profile. The figure shows the temperature profile growing with rising the values of thermophoresis, the figure shows that the boundary layer thickness is enhancing, which leads to the growth in temperature.

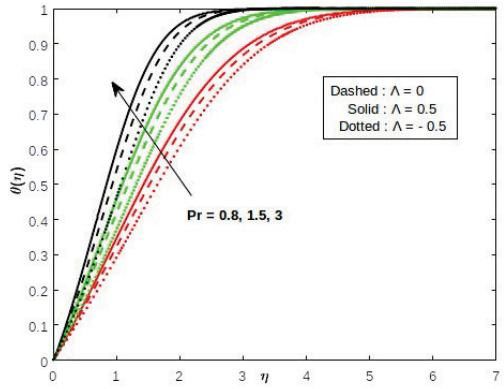

FIGURE 9. Influence of Pr on Temperature for various values of Λ

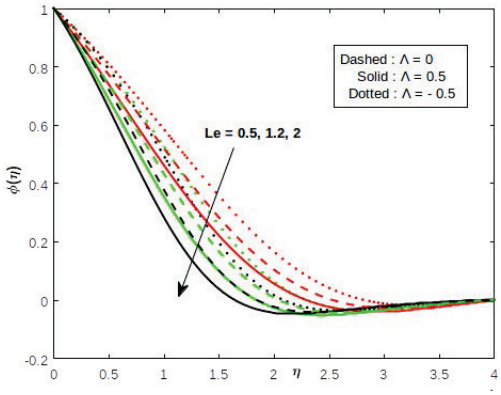

FIGURE 10. Influence of Le on concentration for various values of Λ

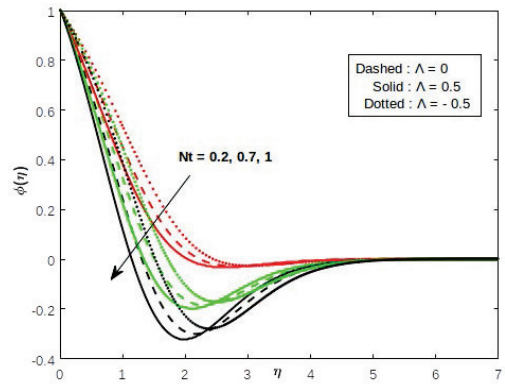

FIGURE 11. Influence of Nt on concentration for various values of Λ

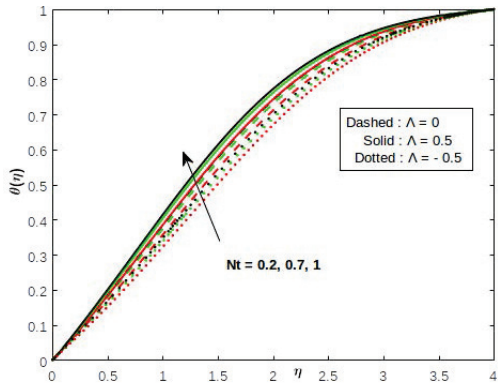

FIGURE 12. Influence of Nt on temperature for various values of Λ

CONCLUSION

- Flow velocity is increase with enhancing the values of wedge angle and magnetic field parameters.

- Thickness of the boundary layer is decline with increasing the magnetic field parameter in wedge positions.
- Flow velocity is decreasing with rising the values of Casson parameter and permeability parameter.
- Skin friction coefficient is enhancing in increase of magnetic field parameter.
- With an increasing of Prandtl Number, temperature profile is increases.
- The values of thermal radiation is growing, found decline the temperature and concentration profile.
- Mass transfer rate increases in all wedge places with a rising the values of the wedge angle, themophoresis, magnetic field and thermal radiation factor.

REFERENCES

[1] A. JAMESON: *Iterative solution of transonic flows over air foils and wings including flows at Match1*, Commun. on Pure and Appl. Math., **27** (1974), 283–309.

[2] M. KUMARI, H. TAKHAR, G. NATH: *Mixed convection flow over a vertical wedge embedded in a highly porous medium*, Heat and Mass Transfer, **37** (2001), 139–146.

[3] W.T.C. CHENG, H. LIN: *Transient mixed convection heat transfer with melting effect from the vertical plate in a liquid saturated porous medium*, Int. J. Eng. and Sci., **44** (2006), 1023-1036.

[4] S.U.S. CHOI, A.J. ESTMAN: *Enhancing thermal conductivity of fluids with nanoparticles. Argone National Lab*, IL(United States), (1995).

[5] R.S.R. GORLA, A. CHAMKHA, A.M. RASHAD: *Mixed convective boundary layer flow over a vertical wedge embedded in a porous medium saturated with a nanofluid*, 3rd Inte. Conf.on Thermal Issues in Emerging Tech. Theory and App., (2011), 445-451.

[6] V.M. FALKNER, S.W. SKAN: *Some approximate solutions of the boundary layer equations*, Philos. Mag., **12** (1931), 865-896.

[7] H.T. LIN, L.K. LIN: *Similarity solutions for laminar forced convection heat transfer from wedge to fluids of any Prandtl number*, Int. J. Heat Mass Tran., **30** (1987), 1111-1118.

[8] R. KANDASAMY, K. PERIASAMY, K.K. SIVAGNANAPRABHU: *Effects of chemical reaction, heat and mass transfer along a wedge with heat source and concentration in the presence of suction or injection*, International Journal of Heat and Mass Transfer, **48**(7) (2005), 1388-1394.

[9] N.G. KAFOUSSIAS, N.D. NANOUSIS: *Magneto hydrodynamic laminar boundary-layer flow over a wedge with suction or injection*, Can. J. Phys., **75**, (1997), 733–745.

[10] I. ULLAH, I. KHAN, S. SHAFIE: *MHD natural convection flow of Casson nanofluid over non linearly stretching sheet through porous medium with chemical reaction and thermal radiation*, Nano scale res. lett., **11** (2016), art.id. 527.

[11] B. SHANKAR GOUD, P. SRILATHA, P. BINDU, Y. HARI KRISHNA: *Radiation effect on MHD boundary layer flow due to an exponentially stretching sheet*, Advances in Mathematics: Scientific Journal, **9**(12) (2020), 10755–10761.

[12] B. SHANKAR GOUD, K. SUDHAKAR REDDY, P. SURESH, M.V. RAMANA MURTHY: *Numerical solution of free convective stratified fluid flow over an infinite vertical porous plate with hall effect*, International Journal of Mechanical and Production Engineering Research and Development, **10**(3) (2020), 10019–10030.

[13] N. KISHAN, C. KALYANI, M. CHENNA KRISHNA REDDY: *MHD boundary layer flow of a nanofluid over an exponentially permeable stretching sheet with radiation and heat source/sink*, Transp. Phenom. Nano. Micro Scales, **4**(1) (2016), 45-51.

[14] B. SHANKAR GOUD: *Thermal radiation influences on MHD stagnation point stream over a stretching sheet with slip boundary conditions*, International Journal of Thermofluid Science and Technology, **7**(2) (2020), Paper No.070201.

[15] ISHAK, A., NAZAR, R., BACHOK, N.: *Melting heat tranfer in steady laminar flow over a moving surface*, Heat and Mass Transfer. **46** (2010), 463-468.

[16] SARKAR, S., ENDALEW, M.F.: *Effects of melting process on the hydromagnetic wedge flow of a Casson nanofluid in a porous medium*, Boundary Value Problems. **2019** (2019), art.id.43.

OSMANIA UNIVERSITY,
DEPARTMENT OF MATHEMATICS,
HYDERABAD, TELANGANA-500007, INDIA.

OSMANIA UNIVERSITY,
DEPARTMENT OF MATHEMATICS,
HYDERABAD, TELANGANA-500007, INDIA.